Cancer Management and Research

Elevate Series

Open Access Full Text Article

ORIGINAL RESEARCH

Tumor-Derived Exosomal PDLIM1 Promotes Angiogenesis and Tumor Progression in Papillary Thyroid Carcinoma: Insights From Integrated Single-Cell Transcriptomics and Exosomal Proteomics

Wangwang Qiu[1,*], Ting Yan[1,2,*], Xinyu Huang[1], Youben Fan[1], Jianzhong Di[1], Zhili Yang[1]

[1]Department of General Surgery, Shanghai Sixth People's Hospital Affiliated to Shanghai Jiao Tong University School of Medicine, Shanghai, 200233, People's Republic of China; [2]Department of General Surgery, Shanghai Fengxian District Central Hospital, Shanghai, 201499, People's Republic of China

*These authors contributed equally to this work

Correspondence: Jianzhong Di; Zhili Yang, Department of General Surgery, Shanghai Sixth People's Hospital Affiliated to Shanghai Jiao Tong University School of Medicine, 600 Yi-Shan Road, Shanghai, 200233, People's Republic of China, Email dijianzhong@sjtu.edu.cn; yangzhililaoshi@126.com

Background: Papillary thyroid carcinoma (PTC) with metastatic potential presents a complex and poorly understood tumor microenvironment. Despite its clinical significance, the cellular and molecular mechanisms driving metastatic progression remain inadequately characterized, particularly the role of intercellular communication mediated by tumor-derived exosomes.

Methods: We analyzed single-cell RNA sequencing (scRNA-seq) on primary and metastatic PTC tissues (n=12 samples from 4 patients), exploring cellular heterogeneity and distinct subpopulations. Metastasis-associated cell states (Scissor+ and Scissor-) were delineated using the Scissor algorithm. Pathway activity in these subpopulations was analyzed using the PROGENy algorithm. Exosomal proteomic data from lymph node metastasis patients were cross-referenced with Scissor+ signatures, identifying candidate proteins. Functional validation included in vitro angiogenesis assays with HUVECs and in vivo xenograft models to assess tumor growth and vascularization.

Results: ScRNA-seq revealed significant tumor cell heterogeneity between primary and metastatic sites, with Scissor+ cells strongly linked to metastatic phenotypes. PROGENy analysis demonstrated significant upregulation of VEGF signaling in Scissor+ cells. Among six key proteins identified, PDLIM1 was highly expressed in PTC cell lines and metastatic tissues ($P < 0.001$). Tumor-derived exosomal PDLIM1 was internalized by endothelial cells, enhancing angiogenesis in vitro. PDLIM1 knockdown in exosomes suppressed HUVEC tube formation ($P < 0.05$) and reduced tumor volume, CD31+ microvessel density, and LYVE-1+ lymphatic vessel density in xenografts ($P < 0.05$).

Conclusion: Our study suggests that exosomal PDLIM1 may play a role in promoting angiogenesis and primary tumor progression in PTC. These findings provide preliminary insights into the potential involvement of exosome-mediated intercellular communication in PTC pathogenesis. Further validation in larger cohorts and functional studies, including rescue experiments, are warranted to evaluate whether targeting PDLIM1 could represent a viable therapeutic strategy.

Keywords: papillary thyroid carcinoma, exosomal proteomics, single-cell transcriptomics, angiogenesis, PDLIM1

Introduction

Thyroid cancer is the most prevalent malignancy of the endocrine system globally, and its incidence in China has shown a significant increase in recent decades.[1,2] Papillary thyroid carcinoma (PTC), which accounts for over 80% of all thyroid malignancies, exhibits a high propensity for cervical lymph node metastasis, with reported rates ranging from 30% to 59.1%.[3,4] Additionally, distant metastasis occurs in approximately 5% to 10% of cases, making it a critical prognostic

https://doi.org/10.2147/CMAR.S589372
Received: 17 December 2025
Accepted: 6 May 2026
Published: 8 May 2026

factor for disease recurrence and patient survival.[4] Nevertheless, the molecular pathogenesis governing PTC metastasis remains incompletely delineated.

Neoplastic lesions typically exhibit a multifaceted tumor microenvironment (TME) composed of heterogeneous cellular constituents, encompassing both malignant cells and non-neoplastic elements such as vascular endothelial cells, cancer-associated fibroblasts (CAFs), and tumor-infiltrating immune cells.[5] These cellular components undergo dynamic evolution under the influence of diverse selective pressures, including nutrient deprivation, metabolic reprogramming, immune surveillance, and therapeutic interventions, culminating in the emergence of complex intratumoral heterogeneity (ITH) that drives malignant progression, metastatic dissemination, and therapeutic refractoriness.[6] Conventional investigations into ITH in advanced PTC have predominantly employed bulk tissue genomic analyses, which yield averaged gene expression signatures without elucidating cell-type-specific transcriptional or proteomic profiles, their relative abundance, or their intricate interplay within the TME.[7]

The advent of single-cell multi-omics technologies has revolutionized oncology research by enabling high-resolution deconvolution of tumor heterogeneity and the architectural complexity of thyroid neoplasms at single-cell resolutions.[8] Contemporary investigations have leveraged single-cell RNA sequencing (scRNA-seq) platforms to dissect the cellular architecture of thyroid malignancies. Our prior scRNA-seq analysis of advanced PTC specimens unveiled distinct ITH patterns within both neoplastic epithelial cell clusters and diverse stromal cell populations, illuminating microenvironmental remodeling during tumor evolution.[9] Complementary studies have corroborated these findings, revealing analogous cellular ecosystems in PTC.[10–13] These collective observations underscore the imperative for comprehensive exploration of the bidirectional signaling networks between neoplastic subclones and their associated stromal or immunomodulatory cell populations within the PTC TME.

Exosomes are membrane-bound extracellular vesicles that encapsulate functional bioactive macromolecules, including miRNAs, lipids, and proteins, which can be transferred to recipient cells while retaining their biological activity.[14,15] The pre-metastatic niche, established prior to the arrival of tumor cells, plays a pivotal role in sustaining the growth of metastatic tumor cells. Tumor-derived exosomes (TDEs) are recognized as critical regulators of pre-metastatic niche formation, as they facilitate dynamic intercellular communication by delivering specific molecular cargo to immune cells and stromal cells.[16] Limited studies have focused on the gene expression profiles and proteomic signatures of PTC with metastasis.[17–19] One such study employed a proteomic approach to compare the protein expression profiles in serum-purified exosomes from PTC patients with metastasis, PTC patients without metastasis, and matched healthy controls.[18] However, these investigations were predominantly based on bulk tissue analyses, leaving unresolved the precise mechanisms by which exosomes derived specifically from tumor cells, rather than the entire tumor mass, mediate PTC metastasis. Integrating single-cell multi-omics approaches to identify and characterize tumor cell-derived exosomes could provide novel therapeutic insights for addressing PTC progression.

PDLIM1, also known as CLP36, Elfin, or CLIM1, is a member of the PDZ-LIM protein family and is implicated in diverse physiological processes, including cytoskeletal regulation and synaptic formation.[20] Accumulated evidence indicates that PDLIM1 is dysregulated in various malignancies and plays a significant role in tumorigenesis and cancer progression, as observed in colorectal cancer,[21] hepatocellular carcinoma,[22] breast cancer,[23] pancreatic cancer,[24] glioma,[25] and chronic myeloid leukemia.[26] Mechanistically, PDLIM1 may contribute to tumorigenesis by modulating cellular proliferation and metastasis. Its dysregulation can lead to aberrant signaling pathways and interactions with proteins such as actin filaments, may be involved in regulating the proliferation, metastasis, and survival of malignant cells, ultimately influencing cancer progression. Additionally, PDLIM1 is involved in the epithelial–mesenchymal transition (EMT), a critical process through which cells acquire migratory and invasive capabilities.[27] As a cytoskeletal protein, PDLIM1 has been shown to participate in EMT across multiple tumor types.[27] Although the upregulation of PDLIM1 protein expression has been reported in PTC,[28] its role and mechanism in PTC metastasis, particularly in the context of exosome-mediated communication, have not been well elucidated.

In this study, we integrated scRNA-seq data from both internal and publicly available datasets with bulk transcriptome data to identify metastasis-associated subpopulations using the Scissor algorithm. We further characterized the functional pathways in these subpopulations. By referencing differentially expressed, tumor-derived, exosome-related genes associated with metastasis, we employed a multi-modal analytical approach to isolate PDLIM1 as a tumor-derived

exosome marker specifically expressed in metastatic PTC. The upregulation of PDLIM1 was subsequently validated in PTC cell lines and tissue cohorts through immunohistochemistry and quantitative reverse transcription PCR (qRT-PCR). Furthermore, in vitro and in vivo functional assays were conducted to investigate the potential role of tumor-derived exosomal PDLIM1 in angiogenesis and tumor progression in PTC.

Materials And Methods

Data Sources

The single-cell RNA sequencing dataset generated in our center (PRJNA766250, n=3 samples) was combined with a publicly available single-cell dataset, obtained from the GEO database (GSE184362, n=9 samples), totaling 12 samples from 4 patients, which includes primary and metastatic PTC samples alongside matched, normal thyroid tissues.[10] Transcriptomic profiles and clinicopathological information for patients with PTC were retrieved from The Cancer Genome Atlas (TCGA) database (https://portal.gdc.cancer.gov/). The exosome dataset was derived from a published study comprising serum-purified exosomes from 16 healthy volunteers, 16 PTC patients with lymph node metastasis (LNM), and 17 PTC patients without LNM.[18] Differentially expressed proteins between LNM and non-LNM groups were identified using a threshold of protein abundance ratio ≥ 1.5 or ≤ 0.5.

Clinical Specimens

The primary tumors, metastatic lesions, and matched normal tissues utilized in this study were obtained from the same individuals. A total of 20 formalin-fixed, paraffin-embedded tissue samples were collected from patients diagnosed with PTC and concurrent LNM at our center between January 2024 and June 2024 for immunohistochemical analysis. All patients, aged 18 to 70 years, had not undergone any prior treatments before surgery. The diagnosis of PTC with cervical lymph node metastasis was confirmed via postoperative pathological examination. This study was approved by the Institutional Ethics Committee of Shanghai Sixth People's Hospital Affiliated to Shanghai Jiao Tong University School of Medicine (Approval No.:2019–146-(3)), and written informed consent was obtained from all participants.

Cell Lines and Animal Models

The normal thyroid follicular cell line Nthy-ori 3–1; PTC cell lines TPC-1, BCPAP, and K1; and human umbilical vein endothelial cells (HUVECs) were obtained from the Cell Bank of the Chinese Academy of Sciences. All cell lines underwent short tandem repeat authentication and mycoplasma contamination testing. Female M-NSG mice (4–6 weeks old) were purchased from Shanghai Model Organisms and were maintained under specific pathogen-free conditions. Animal experiments were approved by the Institutional Animal Care Committee of Shanghai Sixth People's Hospital Affiliated to Shanghai Jiao Tong University School of Medicine (Approval No.: 2022–0110) and were conducted in accordance with the Guide for the Care and Use of Laboratory Animals (8th edition, National Research Council, 2011) as well as the Chinese national standard Guideline for Ethical Review of Laboratory Animal Welfare (GB/T 35892–2018). All animals were euthanized by cervical dislocation at the end of the experiments.

Bulk and scRNA-Seq Data Processing

For the analysis of scRNA-seq data, we employed the Seurat (v4.3.0) R package workflow, which included cell filtering, normalization, dimensionality reduction, and clustering. Batch effects were mitigated using the IntegrateData function based on the Canonical Correlation Analysis (CCA) algorithm. Data processing was performed using Seurat with default settings for quality control. Quality control thresholds were set as nFeature_RNA between 200 and 7500, and percent.mito < 25%. Significant dimensions were identified through Principal Component Analysis (PCA) with a threshold of $P < 0.05$, and dimensionality reduction was achieved by applying Uniform Manifold Approximation and Projection (UMAP) to the top 20 principal components. Cell clusters were identified with the FindClusters function at a resolution of 0.5.

The identification of metastasis-associated, single-cell subpopulations was conducted using the Scissor software (version 2.0.0).[29] For this analysis, the normalized scRNA-seq expression matrix and the bulk RNA-seq data from The Cancer Genome Atlas (TCGA) Thyroid Cancer (THCA) cohort, along with its accompanying lymph node metastasis

(LNM) phenotypic information, were used as inputs. The Scissor algorithm was run with a beta parameter of 0.5, and the phenotype of interest was LNM status. Both the single-cell data (aggregated to pseudo-bulk samples per cell cluster) and the bulk RNA-seq data were normalized to counts per million (CPM) and log2-transformed (logCPM) to minimize technical biases. Pearson correlation coefficients were calculated between each single cell and each bulk sample to estimate their similarity. A Cox regression-based model was then applied to this correlation matrix, with the LNM status as the survival phenotype, to select cell subpopulations most significantly associated with the metastatic outcome. The optimal parameter λ was set to 0.5 to balance model complexity and performance. Cells with positive Scissor associations were defined as metastasis-associated (Scissor+) cells, while those with negative associations were defined as non-metastasis-associated (Scissor-) cells. To further characterize the functional pathways enriched in metastasis-associated subpopulations, we performed pathway activity analysis using the PROGENy algorithm (version 1.16.0).

Cell Culture

The TPC-1, Nthy-ori 3–1, K1, and BCPAP cell lines were cultured in an RPMI-1640 (Gibco, USA) medium supplemented with 10% fetal bovine serum (Gibco, USA) or in a complete medium with exosome-depleted serum (Systembio, China). HUVECs were maintained in an endothelial cell-specific medium (ScienCell, USA). All cells were incubated at 37°C in a humidified atmosphere containing 5% CO2. For subculturing, culture flasks were removed from the incubator, and the medium was aspirated. The cells were washed twice with PBS (Servicebio, China) and then treated with a trypsin solution (Gibco, USA) for 1 minute at 37°C. Detachment was monitored under a microscope, and once the cells assumed a rounded morphology, the trypsin solution was removed. A complete medium was added to neutralize the trypsin, and the cells were gently resuspended by pipetting. Cells were then passaged at a 1:3 ratio for continued cultivation.

qRT-PCR Analysis

Total RNA was extracted from the cells using a TRIzol reagent (Invitrogen, USA) following the manufacturer's protocol. cDNA was synthesized using the PrimeScript™ RT Reagent Kit (Takara, Japan). qRT-PCR was performed using the SYBR Green PCR Master Mix (Applied Biosystems, USA) in a 20 μL reaction volume containing target gene primers, cDNA, and nuclease-free water. The amplification protocol included an initial denaturation step at 95°C for 30 seconds, followed by 40 cycles of denaturation at 95°C for 10 seconds and annealing/extension at 70°C for 10 seconds. The housekeeping genes β-actin and U6 were used as internal controls, and the relative expression levels of the target genes were calculated using the $2^{(-\Delta\Delta Ct)}$ method. Each experiment was performed in triplicate. The PCR primer sequences for the target genes are listed in Table 1.

Immunohistochemical Staining and Scoring

Paraffin-embedded PTC tissue sections were deparaffinized, rehydrated, and subjected to antigen retrieval in citrate buffer (pH 6.0) using microwave heating at 98°C for 20 minutes. Endogenous peroxidase activity was blocked with 3% hydrogen peroxide, followed by blocking with 5% bovine serum albumin (Beyotime, China). Sections were incubated overnight at 4°C with the primary antibody against PDLIM1 (Abclonal, China), diluted according to the manufacturer's instructions, and then with a horseradish peroxidase (HRP)-conjugated secondary antibody (Beyotime, China) for 1 hour at 37°C. Color development was performed using a DAB Substrate Kit (Beyotime, China), and nuclei were counterstained with DAPI (Servicebio, China). After dehydration and mounting, staining was evaluated based on intensity (0:

Table 1 Primer Sequences for qRT-PCR Analysis

Gene	Forward (5′→3′)	Reverse (5′→3′)
PDLIM1	CGATTGGAAATGCTCAGAAGTTGCC	TTTCAGGTTGGTGCCACAGTCAG
SRGN	TTCCAGGTGAATCCAACAAGATCCC	AGCCGAAGCCTGATCCAGAGTAG
TXN	GGTGAAGCAGATCGAGAGCAAGAC	CATTTTGCAAGGCCCACACCAC
ALDOA	ACCGAGAACACCGAGGAGAACC	TCATCCGCCTTCTGGTAGAGTGTC
ATP5B	GTTGGCAGTGAGCATTACGATGTTG	GCACGGGACACGGTCAACTTG

negative; 1: weak; 2: moderate; 3: strong) and the percentage of positively stained cells (1: <25%; 2: 25–50%; 3: 50–75%; 4: >75%). The final score was calculated by multiplying the intensity and percentage scores.

Western Blotting

Protein was extracted from cells or exosomes using RIPA buffer (Thermo Fisher Scientific, USA) supplemented with a PMSF protease inhibitor. Protein concentration was determined using a BCA Protein Assay Kit (Beyotime, China), with absorbance measured at 562 nm. Samples were denatured, separated on a 12% SDS-PAGE gel, and transferred to a PVDF membrane (Millipore, USA) at 100 V for 40 minutes. The membrane was blocked with 5% non-fat milk and incubated with the primary antibody overnight at 4°C, subsequently being incubated with an HRP-conjugated secondary antibody for 1 hour at room temperature. Protein bands were visualized using ECL substrate (NCM Biotech, China) and a chemiluminescence imaging system (Bio-Rad, USA).

Exosome Isolation and Transmission Electron Microscopy (TEM) Analysis

Exosomes were isolated from PTC cell lines cultured in an exosome-depleted, complete medium for 48 hours. The supernatant was filtered through a 0.22 μm sterile filter and subjected to sequential centrifugation (300 × g for 10 minutes, 3,000 × g for 10 minutes, and 10,000 × g for 10 minutes at 4°C), followed by ultracentrifugation at 110,000 × g for 90 minutes at 4°C. The exosome pellet was resuspended in PBS and stored at −80°C or used for TEM, Western blot, and tracking experiments. For TEM analysis, exosomes were fixed with 2.5% glutaraldehyde, loaded onto a formvar/carbon-coated copper grid, stained with 3% phosphotungstic acid, and examined under a TEM (Hitachi, Japan) at 80 kV.

Exosome Uptake Assay

For uptake experiments, exosomes were fluorescently labeled using the PKH26 linker dye (Umibio, China) according to the manufacturer's instructions. Briefly, the PKH26 linker was mixed with Diluent C at a 1:9 ratio under light-protected conditions to prepare the staining solution. Freshly isolated exosomes were incubated with the staining solution, gently mixed, and incubated in the dark for 10 minutes. Excess dye was removed by washing with PBS to avoid overstaining. HUVECs were seeded in confocal dishes (Nest, China) one day prior to the experiment. The labeled exosomes were added to the adherent HUVECs and incubated for 2 hours in a cell culture incubator. Exosome uptake by the cells was visualized and documented using laser confocal microscopy (Leica, Germany).

Tube Formation Assay

A Matrigel matrix (Corning, USA) was thawed overnight at 4°C, and a 24-well plate (Corning, USA) was prepared by adding 200 μL of liquefied Matrigel to each well, followed by incubation at 37°C for 30 minutes to allow for solidification. After gelation, cell suspensions mixed with the conditioned medium from the PTC cells were added to the Matrigel-coated wells at a density of 1×10^4 cells per well. The plate was gently shaken and incubated for 4 hours at 37°C. Tube formation was then observed and imaged under a microscope (Nikon, Japan).

Lentiviral Transfection and siRNA Interference

Lentiviral transfection was performed according to the manufacturer's instructions. Cells were cultured under standard conditions (37°C, 5% CO_2, 95% humidity). At the logarithmic growth phase, the cells were digested and resuspended as a single-cell suspension. Then, the cells were seeded in a 96-well plate and incubated overnight. A concentration gradient was established to determine the optimal multiplicity of infection (MOI), with 80% cell infection efficiency as the criterion. The optimal MOI for PTC cells was determined to be 20. Polybrene (Beyotime, China) was added to enhance transfection efficiency, and stable transfected cells were selected using puromycin (Yeason, China). The cells were divided into three groups: a control group (CON) with no treatment, a negative control group (NC) with a non-targeting siRNA, and a siRNA targeting PDLIM1 group, where PDLIM1 was knocked down (KD). Lentiviral vectors for KD and negative control NC were purchased from Shanghai GeneChem (China). The target sequences for si-PDLIM1 were as follows: KD1: GCTCAGAAGTTGCCTATGTGT; KD2: GCCTTGTCATCGACAAAGAAT; KD3: GCCTTGGTTAATTGACTCACA. The si-NC target sequence was TTCTCCGAACGTGTCACGT.

Xenograft Models

TPC-1 cell lines were cultured and harvested during the logarithmic growth phase. Cells were trypsinized (Gibco, USA), centrifuged at 1000 rpm for 5 minutes, washed twice with PBS, and resuspended to a concentration of 1×10^7 cells/mL. The cell suspension was mixed with the pre-chilled Matrigel matrix solution (Corning, USA) at a 1:1 ratio on ice to prevent premature gelation. A 100 μL mixture (1×10^6 cells/mouse) was subcutaneously injected into the axillary region of 6-week-old female M-NSG mice (Shanghai Model Organisms Center, China). Tumor volumes were measured every 3 days, starting first week post-injection, using a caliper and were calculated using the formula $V = ab^2/2$, where "a" and "b" represent tumor length and width, respectively. At the fourth week post-implantation, the mice were intravenously injected with 150 mg/kg pentobarbital sodium for euthanasia. Tumors were excised, photographed, and divided for further analysis; one portion was snap-frozen in liquid nitrogen for molecular studies, and the other was fixed in 4% paraformaldehyde (Servicebio, China) for paraffin embedding and histological examination.

Statistical Analysis

All data are presented as the mean ± standard deviation from three independent experiments. For comparisons between two groups, an unpaired Student's *t*-test was used. For comparisons among three or more groups, one-way analysis of variance (ANOVA) was performed, followed by Tukey's post-hoc test for multiple comparisons in GraphPad Prism 7 (GraphPad Software, USA). Significance levels are denoted by asterisks, as follows: *P < 0.05, **P < 0.01, and ***P < 0.001.

Results

Cellular Atlas of Primary and Metastatic PTC

To explore the cellular composition of PTC tissues with metastasis, we examined 12 samples from four patients with PTC, covering primary tumors, metastatic tumors, and corresponding normal thyroid tissues. These samples were collected from our center and supplemented with publicly available scRNA-seq data (PRJNA766250 and GSE184362). After rigorous quality checks and filtering, we identified 76,489 high-quality cells (Figure 1A and B). Following normalization and integration to eliminate batch effects, the data revealed three distinct clusters: 9,278 epithelial cells, 5,538 stromal cells (including 4395 fibroblast cells and 1143 endothelial cells), and a striking 61,673 immune cells. This highlights the finding that immune cells made up 80% of the total cell population, dominating both normal and tumor tissues (Figure 1C and D).

Transcriptional Profiles of Primary and Metastatic PTC Tumor Cells

To avoid clustering artifacts caused by data integration, we re-clustered epithelial cells to accurately identify subpopulations (Figure 2A). Given their common epithelial origin, both normal follicular epithelial cells and tumor cells expressed epithelial markers. To distinguish between normal and tumor cells, we used two additional markers, TPO and SLC26A4, to identify C1, C2, and C3 as normal follicular epithelial cells (Figure 2C). These markers were previously shown to be expressed in normal thyroid tissues but absent in tumor cells. Tumor cells were primarily clustered by primary and metastatic samples, indicating significant heterogeneity between the two phenotypes (Figure 2B). We further employed bulk data and phenotypic information to assist in single-cell data analysis using the Scissor algorithm, identifying the cell subpopulations most highly associated with the metastatic phenotype. The results revealed the presence of Scissor+ cells (metastasis-related) and Scissor-cells (metastasis-unrelated) within the tumor cell population (Figure 2D). Pseudotime trajectory analysis showed no overlap between Scissor+ and Scissor- cells, suggesting distinct cellular states (Figure 2E). To gain functional insights into the characteristics of metastasis-associated subpopulations, we analyzed pathway activity in Scissor+ and Scissor- cells using the PROGENy algorithm. This analysis revealed significant pathway dysregulation in the metastasis-associated subpopulation. Specifically, Scissor+ cells exhibited marked upregulation of VEGF signaling, along with significant activation of Androgen and TGFb pathways compared to Scissor- cells (Figure 2F). Considering the fact that RNA sequencing results may not fully represent post-transcriptional and post-translational regulatory changes, we cross-referenced differentially expressed proteins in blood exosomes from LNM patients with the

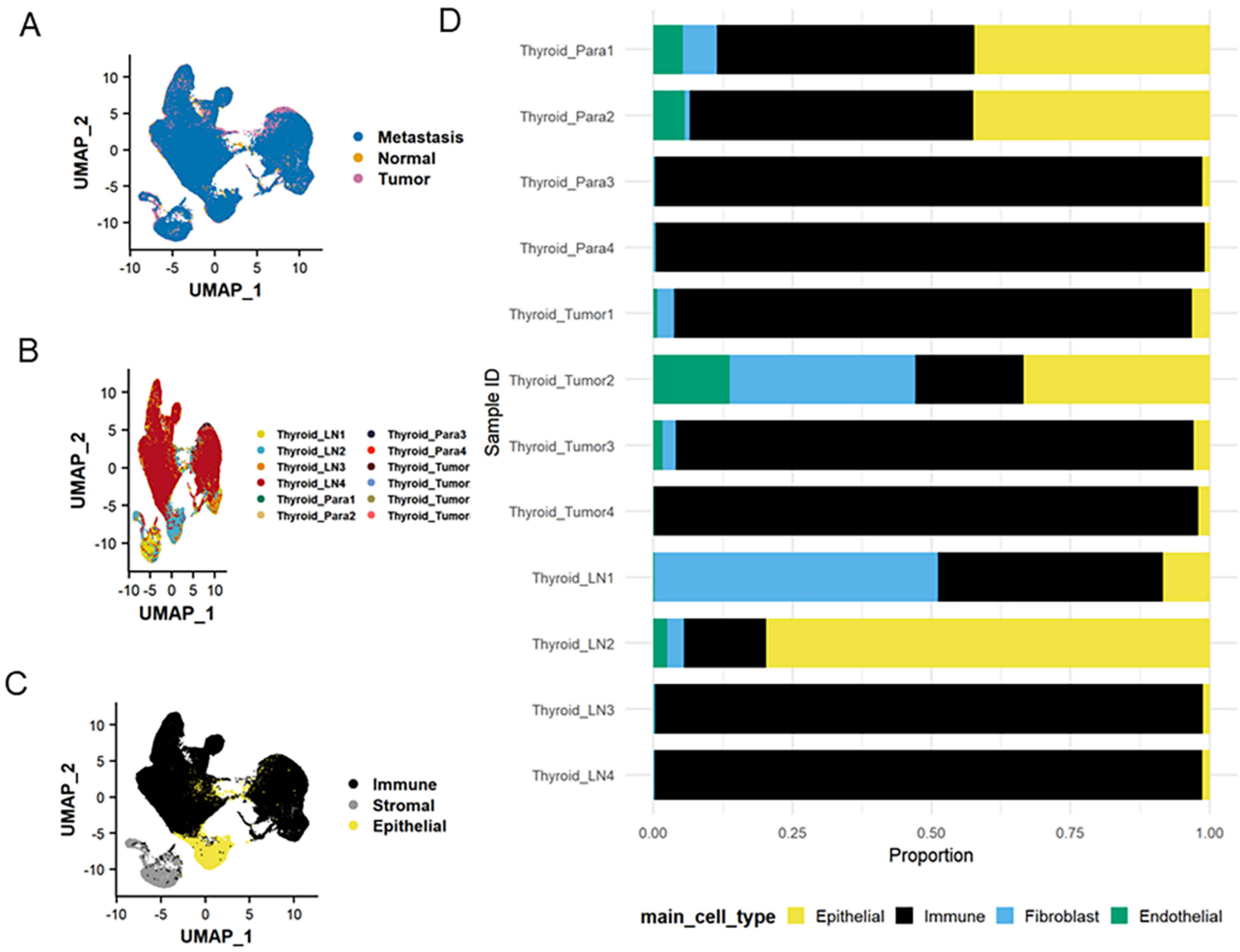

Figure 1 Single-cell transcriptomic profiling of primary, metastatic, and adjacent normal tissues in papillary thyroid carcinoma. (**A**) UMAP visualization stratified by tissue compartment as follows: primary tumor, lymph node metastasis, and matched adjacent normal tissue. (**B**) UMAP visualization stratified by individual sample IDs. (**C**) Cell type classification revealing four dominant populations: epithelial cells, immune cells, fibroblast cells, and endothelial cells. (**D**) Proportional distribution of cell types across samples.

characteristic genes of Scissor+ cell subpopulations, identifying the following six key proteins: TXN, SRGN, PDLIM1, GNAQ, ATP5B, and ALDOA (Figure 2G).

PDLIM1 Is Highly Expressed in PTC Cancer Cells and Metastatic Tissues

qRT-PCR results showed that PDLIM1 expression was significantly elevated in three PTC cell lines compared to normal thyroid follicular epithelial cells ($P < 0.001$; Figure 3A). Immunohistochemistry (IHC) analysis of PTC tissue cohorts revealed that PDLIM1 expression was localized to malignant follicular epithelial cells in PTC. Additionally, IHC scores were significantly higher in metastatic PTC tissues compared to adjacent normal tissues and primary PTC tissues ($P < 0.001$; Figure 3B and C).

PDLIM1 Is Transferred to Endothelial Cells via Exosome Secretion

Exosomes were isolated and purified from conditioned media of PTC cell lines K1 and TPC-1 using standard ultracentrifugation methods. Electron microscopy confirmed the cup-shaped morphology of the isolated exosomes (Figure 4A). The presence of exosome-specific markers TSG101 and CD63 further validated the exosomes, and PDLIM1 protein was detected in exosomes from both cell lines (Figure 4B). To assess exosome delivery, tumor-derived exosomes were labeled with PKH26 (red) and incubated with human umbilical vein endothelial cells

https://doi.org/10.2147/CMAR.S589372

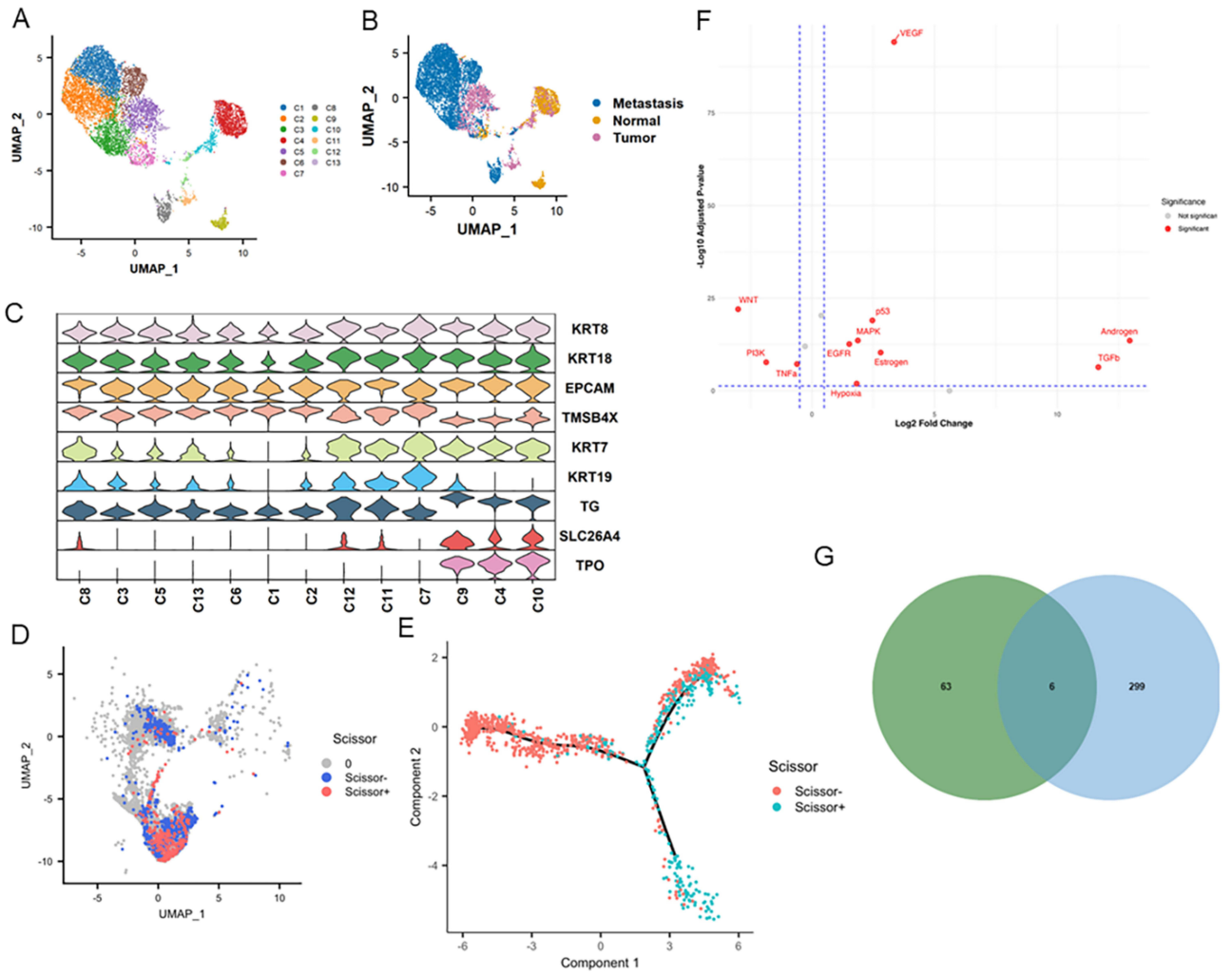

Figure 2 Single-cell resolution of epithelial cell heterogeneity in papillary thyroid carcinoma. (**A**) Unsupervised clustering identifying 13 transcriptionally distinct epithelial subpopulations (C1-C13). (**B**) Compartment-specific distribution of epithelial subclusters across tissue types, as follows: primary tumor, metastasis, and adjacent normal. (**C**) Violin plots confirming the differential expression of pan-epithelial markers. (**D**) Identification of metastasis-associated epithelial subpopulations using the Scissor algorithm. The UMAP projection shows epithelial cells colored by their Scissor phenotype. The analysis was performed with $\lambda = 0.5$. (**E**) Integration of Scissor algorithm with pseudotime trajectory analysis, revealing two malignant evolutionary paths. (**F**) PROGENy pathway activity analysis showing significant upregulation of VEGF, Androgen, and TGFb pathways in Scissor+ compared to Scissor- cells. (**G**) Intersection analysis of differentially expressed proteins in blood exosomes from LNM patients with signature genes of Scissor+ cell subpopulations.

Abbreviation: LNM, lymph node metastasis.

(HUVECs). Confocal imaging revealed PKH26-labeled exosomes within recipient endothelial cells, confirming the transfer of tumor-derived exosomes to endothelial cells (Figure 4C).

Tumor-Derived Exosomal PDLIM1 Regulates HUVEC Angiogenesis in vitro

To investigate the biological function of tumor-derived exosomal PDLIM1 in endothelial cells, TPC-1 cells were stably transfected with siRNA, targeting PDLIM1 to establish a knockdown (KD) model. Western blot analysis demonstrated a significant reduction in PDLIM1 expression in the KD group (siRNA targeting PDLIM1), confirming the efficiency of the knockdown (Figure 5A). For subsequent experiments, the KD2 target was selected based on its robust knockdown efficacy. Importantly, the expression of PDLIM1 in exosomes isolated from the KD group was also markedly reduced, consistent with the cellular knockdown results (Figure 5B), thereby validating the successful suppression of PDLIM1 in both cellular and exosomal compartments. Angiogenesis assays were performed to evaluate the effect of tumor-derived exosomal PDLIM1 on endothelial tube formation. HUVECs were treated with conditioned media from the Control (CON) group (no treatment), Negative control (NC) group (non-targeting siRNA), and KD groups, and the results

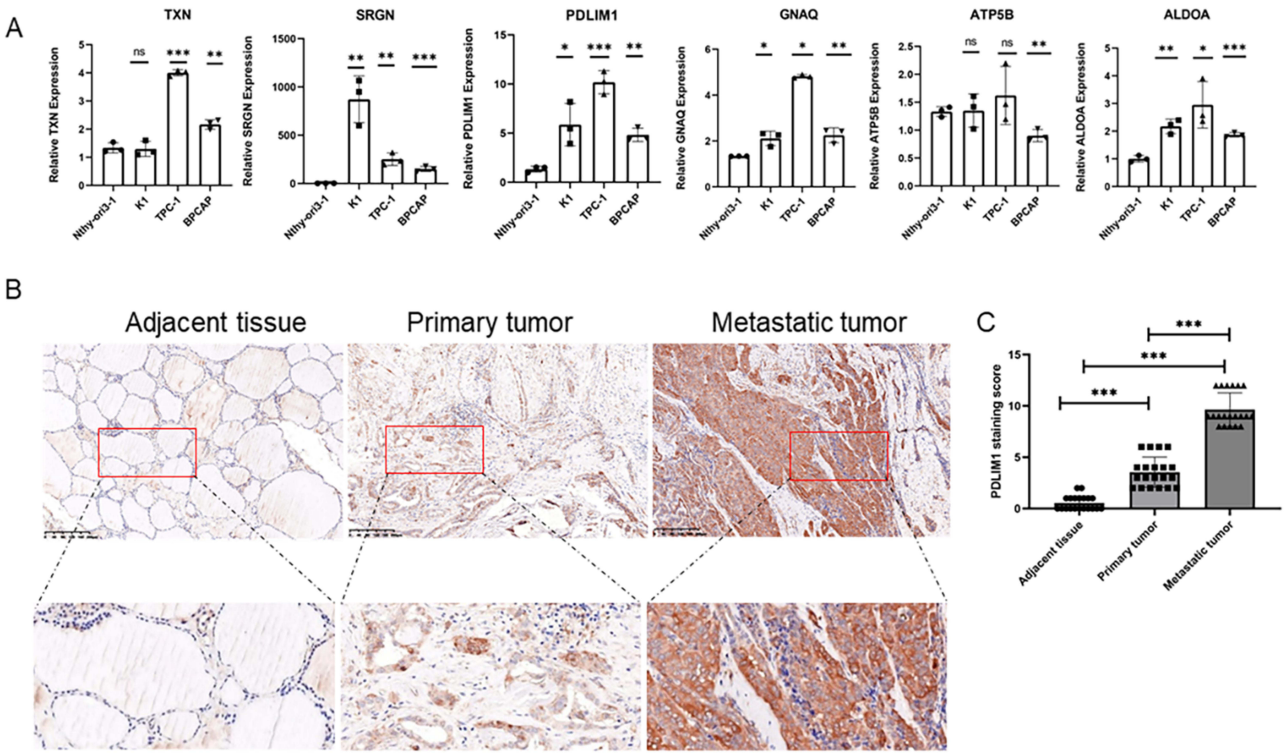

Figure 3 Expression of PDLIM1 in PTC cells and tissues. (**A**) Relative RNA expression levels of six differentially expressed genes. (**B**) Expression profiling of PDLIM1 in primary PTC, lymph node metastasis, and adjacent normal thyroid tissues. Rectangular dashed boxes indicate the areas shown at higher magnification in the adjacent insets. (**C**) Immunohistochemical scoring of PDLIM1 expression. Statistical significance was determined by one-way ANOVA. ***P < 0.001, **P < 0.01, *P < 0.05.
Abbreviation: ns, not significant.

showed that HUVECs treated with KD exosomes exhibited significantly reduced tube formation compared to those treated with CON and NC exosomes (***P < 0.001) (Figure 5C and D).

Tumor-Derived Exosomal PDLIM1 May Functionally Contribute to Both Pathological Angiogenesis and Neoplastic Cell Expansion in vivo

Subcutaneous tumor formation experiments were performed in M-NSG mice using NC and si-PDLIM1 KD cells. Tumor growth in the KD group was slower and significantly smaller compared to the NC group (Figure 6A). Quantitative tumor growth curves demonstrated markedly elevated tumor volumes and accelerated growth rates in NC-implanted mice compared to the KD cohort (P < 0.05, Figure 6B). Immunohistochemical staining of CD31 in the harvested tumor specimens indicated a statistically significant increase in microvascular density (CD31-positive cell ratio) within NC-derived tumors relative to their KD counterparts (P < 0.05), confirming that tumor-derived exosomal PDLIM1 promotes angiogenesis and tumor growth (Figure 6C and D). Immunohistochemical analysis of the lymphatic endothelial marker LYVE-1 on tumor specimens showed markedly reduced lymphatic vessel density in the PDLIM1-knockdown group compared to controls (Supplementary Figure 1).

Discussion

This study offers preliminary insights into the cellular and molecular mechanisms underlying tumor progression in PTC using an integrated multi-omics approach. Using scRNA-seq data, we examined 76,489 single cells from 12 samples of four patients with advanced PTC, covering primary tumors, metastases, and matched adjacent tissues. The re-clustering of epithelial cells revealed significant heterogeneity between primary and metastatic PTC, highlighting the dynamic nature of tumor evolution. This analysis unveiled the diverse cellular landscape within tumors. Using unique gene markers, epithelial cells were grouped into 13 clusters: 3 normal epithelial groups and 10 cancer cell groups.

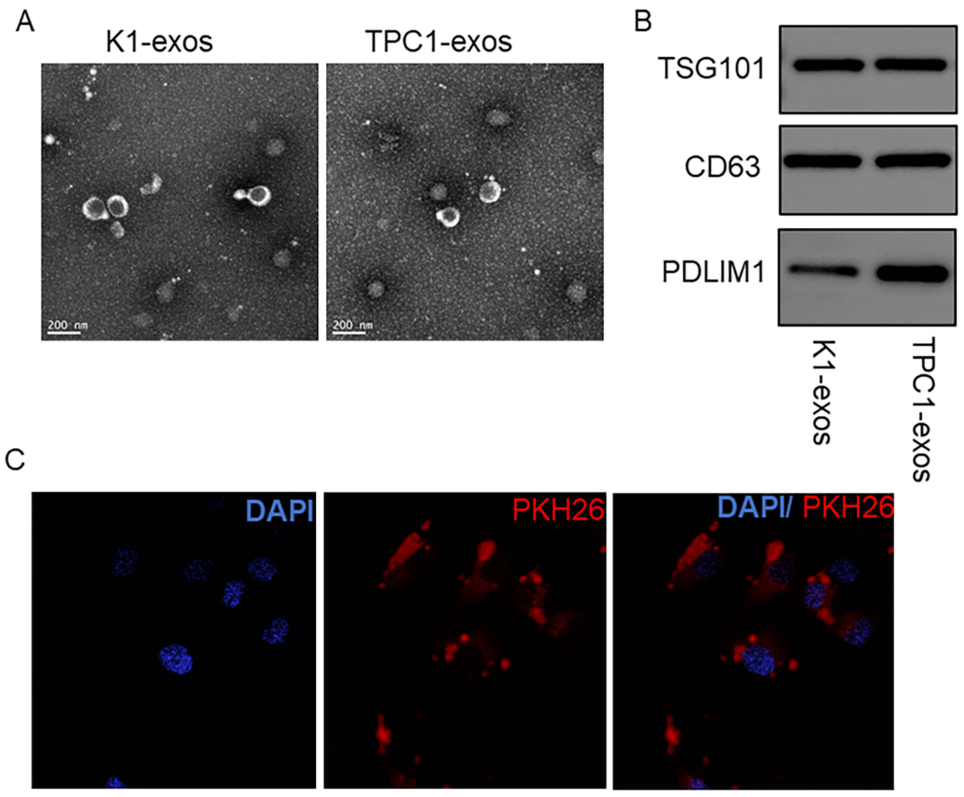

Figure 4 Identification and uptake of tumor-derived exosomes. (**A**) Electron microscopy of exosomes isolated from K1 and TPC-1 conditioned media. (**B**) Western blot analysis of exosomal markers and PDLIM1. (**C**) Confocal microscopy images demonstrating the uptake of PKH26-labeled (red) tumor-derived exosomes by human umbilical vein endothelial cells (HUVECs). Cell nuclei are stained with DAPI (blue). The merged image shows the intracellular localization of the exosomes within the recipient cells.

In most solid tumors, when cancer cells overcome evolutionary hurdles to form a group with full metastatic capabilities, they are termed metastasis-initiating cells (MICs). These cells either arise from specific genetic variations in the primary tumor or adapt dynamically to achieve a metastatic state.[30] To understand the behavior of PTC cancer cells, we used the Scissor algorithm, combining phenotypic and bulk omics data to pinpoint biologically and clinically relevant cell groups from single-cell analysis.[29] The Scissor algorithm further delineated metastasis-related (Scissor+) and metastasis-unrelated (Scissor-) cell states, supported by pseudotime trajectory analysis, which showed distinct cellular trajectories. To functionally characterize these states, we performed pathway activity analysis using the PROGENy algorithm, which revealed that Scissor+ cells exhibited significant upregulation of key oncogenic pathways, most notably VEGF signaling, alongside Androgen and TGFb pathways. This finding not only suggests the existence of distinct molecular features in metastatic PTC cells but also points to the activation of a pro-angiogenic program as a core component of their functional identity. Combining single-cell and bulk tissue data, we found a cell group in PTC cancer cells tied to metastasis, aligning with the concept of MICs. The discovery that these cells possess intrinsically active VEGF signaling provides a mechanistic basis for their capacity to drive blood vessel formation, a critical step in the metastatic cascade. Clinically, metastasis stems from MICs, which adapt to specific tumor environments, enabling them to colonize and grow in distant organs through processes such as regeneration, blood vessel formation, and immune suppression.[31]

Exosomes, measuring 30–100 nm, are released into the extracellular space by fusing with the cell membrane and hold promise as biomarkers, therapeutic agents, and molecular carriers.[32–34] Exosomes are now recognized as key players in cell-to-cell communication. The tumor microenvironment, a dynamic system driven by cell interactions, plays a role in tumor growth and spread. Many studies highlight the role of exosomes in regulating the tumor microenvironment, driving metastasis and progression.[35] Endothelial cells, as a critical component of the tumor microenvironment, actively participate in these interactions, regulating tumor angiogenesis, vascular permeability, and immune cell recruitment.[36]

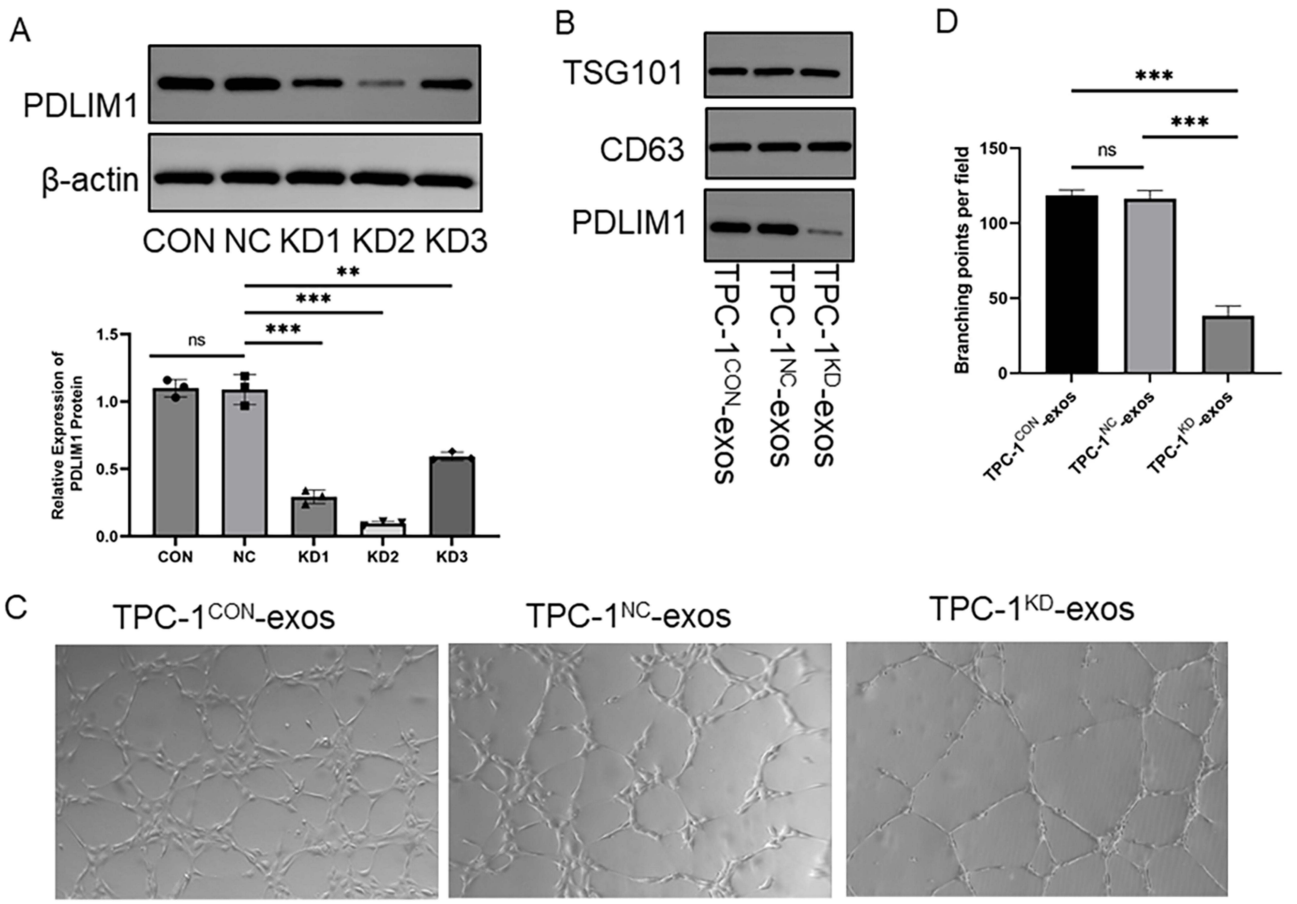

Figure 5 Functional role of tumor-derived exosomal PDLIM1 in endothelial angiogenesis. (**A**) Western blot analysis of PDLIM1 knockdown efficiency in TPC-1 cells. (**B**) Western blot analysis of PDLIM1 in exosomes of TPC-1 cells. Representative images (**C**) and quantitative analysis (**D**) of endothelial tube formation of HUVECs are shown. Statistical significance was determined by one-way ANOVA. *** $P < 0.001$, ** $P < 0.01$.

Abbreviations: ns, not statistically significant; CON, Control group (no treatment); NC, Negative control group (non-targeting siRNA); KD, Knockdown group (siRNA targeting PDLIM1).

Thus, exploring exosome-mediated tumor–endothelial interactions is crucial. Here, we combined single-cell data with TCGA bulk data on metastasis, used Scissor to identify metastasis-related cell groups in PTC, and uncovered unique gene markers for these cells. Using public PTC metastasis-related exosome data, we identified upregulated exosomal proteins in this group, including TXN, SRGN, PDLIM1, GNAQ, ATP5B, and ALDOA. Among the key findings, PDLIM1 emerged as a potential contributor in PTC progression. Its elevated expression in PTC cell lines and metastatic tissues, as confirmed via qRT-PCR and IHC, suggests its potential as a biomarker for aggressive disease. The detection of PDLIM1 in tumor-derived exosomes and its efficient transfer to endothelial cells further implicates exosome-mediated intercellular communication in PTC metastasis.

Functional assays demonstrated that exosomal PDLIM1 significantly enhances endothelial angiogenesis in vitro, while its knockdown impairs tube formation in HUVECs. In vivo experiments using xenograft models provided additional evidence for the pro-tumorigenic and angiogenic effects of exosomal PDLIM1. Mice injected with PDLIM1-knockdown cells exhibited slower tumor growth and reduced angiogenesis, as evidenced by lower CD31 expression. These findings are consistent with a role for PDLIM1 in creating a pro-angiogenic tumor microenvironment, a well-established prerequisite for the metastatic cascade. These results corroborate the in vitro findings and suggest that PDLIM1 may be a potential target for further investigation. The prognosis of patients with metastatic thyroid disease remains challenging to predict, as surgical outcomes can vary significantly across different clinical contexts.[37] Our identification of exosomal PDLIM1 as a pro-angiogenic factor may help address this clinical gap by providing

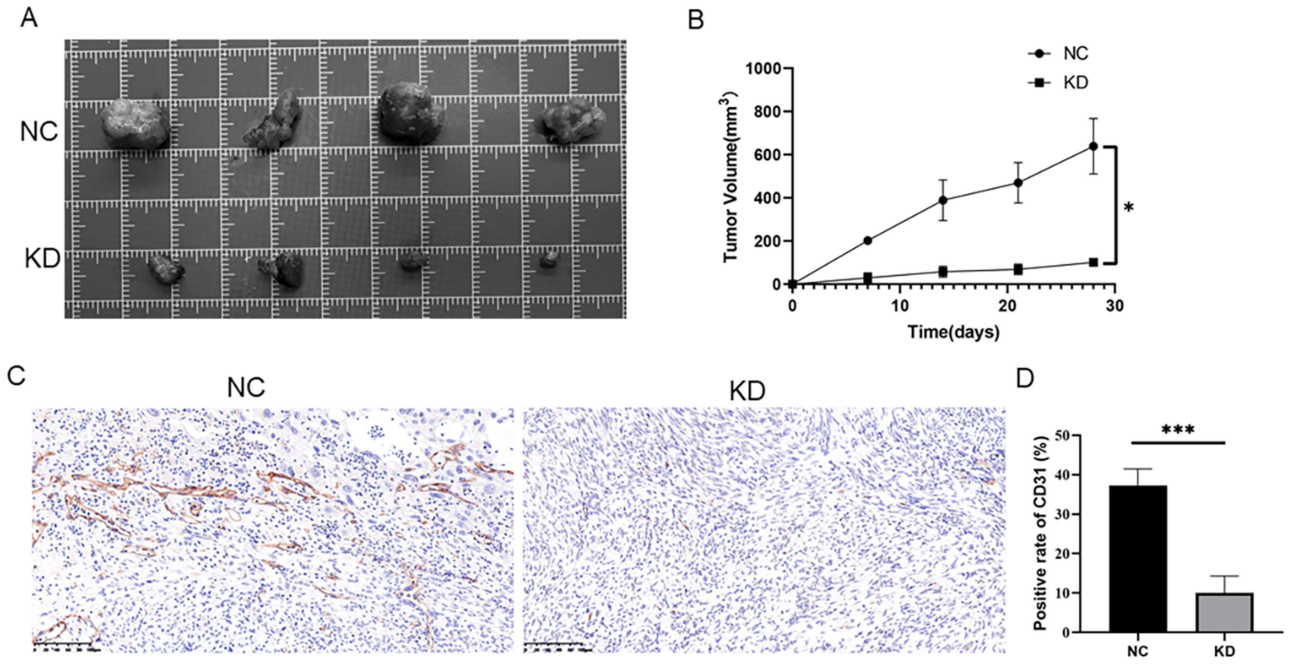

Figure 6 Tumor-derived exosomal PDLIM1 promotes angiogenesis and tumor growth in vivo. (**A**) Subcutaneous tumor formation in M-NSG mice (n=4). (**B**) Quantitative analysis of tumor growth over time. (**C**) Immunohistochemical staining of CD31 in tumor specimens. (**D**) Quantitative analysis of microvascular density (CD31-positive cell ratio) in NC-derived tumors compared to KD-derived tumors. Statistical significance was determined by unpaired Student's *t*-test.*** P < 0.001, * P < 0.05.
Abbreviations: NC, Negative control group (non-targeting siRNA); KD, Knockdown group (siRNA targeting PDLIM1).

a biomarker to identify patients at higher risk of aggressive tumor progression. Moreover, these findings align with previous studies emphasizing the role of exosomes in modulating the tumor microenvironment and promoting metastasis.

Previous studies have implicated PDLIM1 in various signaling pathways, including NF-κB,[38] Wnt/β-catenin,[39] and Hippo,[40] across different cancer types. PDLIM1 mainly interacts with proteins such as actin filaments, influencing cancer cell growth, spread, and survival, as well as ultimately driving cancer progression.[41] Tumor cells gain mobility and invasiveness through EMT, a process involving cytoskeleton reorganization. As a cytoskeletal protein, PDLIM1 is involved in EMT across various cancers.[21] Our findings suggest that PDLIM1 may play a role in regulating angiogenesis. This adds to the growing body of evidence linking exosomal proteins to tumor vascularization.

In the tumor metastasis ecosystem, growing evidence points to endothelial cells as being key players in tumor spread.[42,43] Exosome secretion is a major method by which tumors induce systemic changes, raising questions about their role in blood vessel formation. To investigate this, we isolated exosomes from thyroid cancer cell lines using ultra-centrifugation. Our in vitro uptake assay demonstrated that fluorescently labeled tumor-derived exosomes can be internalized by cultured blood endothelial cells (HUVECs). However, we acknowledge that the in vivo uptake of circulating exosomes in the lymph node pre-metastatic niche is complex and is predominantly mediated by lymphatic endothelial cells and macrophages, with minimal uptake by blood endothelial cells.[44,45] Therefore, the physiological relevance of our in vitro finding warrants further investigation in vivo. To investigate the potential impact of PDLIM1 on the lymphatic system, a key route for PTC metastasis, we performed immunohistochemical analysis of the lymphatic endothelial marker LYVE-1 on the harvested tumor specimens. The density of LYVE-1^{+} lymphatic vessels was markedly reduced in the PDLIM1-knockdown group compared to the control groups (Supplementary Figure 1), suggesting that tumor-derived exosomal PDLIM1 may also facilitate lymphangiogenesis. In vitro and in vivo experiments demonstrated that the exosomal gene PDLIM1 facilitates angiogenesis in PTC. However, the downstream signaling pathways through which exosomal PDLIM1 promotes angiogenesis remain to be fully elucidated. Our PROGENy pathway analysis identified upregulation of VEGF signaling in Scissor+ cells, suggesting a potential link between PDLIM1 and pro-angiogenic pathways. Nevertheless, direct evidence of molecular interactions is lacking and warrants future investigation. Our findings suggest a potential communication pathway between metastasis-associated tumor cells and endothelial cells

via exosomal PDLIM1. The interaction between tumor cells and endothelial cells via exosomes may provide insights into PTC progression. The elevated expression of PDLIM1 in metastatic tissues and its association with angiogenesis suggests that it could be further investigated as a potential biomarker for aggressive PTC.

Several limitations of this study should be acknowledged. First, the sample size for scRNA-seq analysis was relatively small (n=4 patients), which may limit the generalizability of the findings. Second, a key experimental limitation is our use of a subcutaneous xenograft model, which does not directly recapitulate the metastatic cascade. Third, we did not perform rescue experiments to confirm that the observed angiogenic effects are specifically attributable to exosomal PDLIM1 rather than off-target effects of siRNA or other exosomal cargo changes. Fourth, the downstream signaling pathways through which exosomal PDLIM1 promotes angiogenesis and lymphangiogenesis remain to be fully elucidated. Future studies incorporating reconstitution of PDLIM1 in knockdown exosomes are warranted to establish causality.

Conclusion

In conclusion, our integrated analysis suggests that exosomal PDLIM1 may contribute to angiogenesis and primary tumor progression in PTC. These findings offer preliminary insights into potential molecular mechanisms underlying PTC progression. Further validation in larger independent cohorts and functional studies are required before definitive conclusions can be drawn or therapeutic applications considered.

Abbreviations

The following abbreviations are used in this manuscript: PTC, Papillary thyroid carcinoma; ScRNA-seq, Single-cell RNA sequencing; TME, Tumor microenvironment; CAFs, Cancer-associated fibroblasts; ITH, Intratumoral heterogeneity; TDEs, Tumor-derived exosomes; EMT, Epithelial–mesenchymal transition; qRT-PCR, Quantitative reverse transcription PCR; TCGA, The Cancer Genome Atlas; LNM, Lymph node metastasis; CCA, Canonical Correlation Analysis; PCA, Principal Component Analysis; UMAP, Uniform Manifold Approximation and Projection; TEM, Transmission electron microscopy; IHC, Immunohistochemistry; CON, Control; NC, Negative control; KD, Knockdown; MICs, Metastasis-initiating cells; MOI, Multiplicity of infection.

Data Sharing Statement

The datasets used and/or analyzed during the current study are available from the corresponding author, Prof.Zhili Yang, upon reasonable request.

Ethics Approval and Consent to Participate

The study was conducted in accordance with the Declaration of Helsinki and approved by the Ethics Committee of Shanghai Sixth People's Hospital Affiliated to Shanghai Jiao Tong University School of Medicine (2019-146-(3)). The animal study protocol was approved by the Ethics Committee of Shanghai Sixth People's Hospital Affiliated to Shanghai Jiao Tong University School of Medicine (2022-0110) and was conducted in accordance with the Guide for the Care and Use of Laboratory Animals (8th edition, National Research Council, 2011) and the Chinese national standard Guideline for Ethical Review of Laboratory Animal Welfare (GB/T 35892-2018).

Acknowledgments

The authors would like to express their gratitude to the Diabetes Research Institute for the provision of the Beckman ultracentrifuge.

Author Contributions

All authors made a significant contribution to the work reported, whether that is in the conception, study design, execution, acquisition of data, analysis and interpretation, or in all these areas; took part in drafting, revising or critically reviewing the article; gave final approval of the version to be published; have agreed on the journal to which the article has been submitted; and agree to be accountable for all aspects of the work.

Funding

This research was funded by the Project from Shanghai Sixth People's Hospital (grant number YNLC201905), and the Key Medical Disciplines of Shanghai Municipal Health Commission (2024ZDXK0045).

Disclosure

The authors report no conflicts of interest in this work.

References

1. Han B, Zheng R, Zeng H. et al. Cancer incidence and mortality in China, 2022. *J Natl Cancer Center*. 2024;4(1):47–53. doi:10.1016/j.jncc.2024.01.006
2. Siegel RL, Kratzer TB, Giaquinto AN, Sung H, Jemal A. Cancer statistics, 2025. *CA Cancer J Clin*. 2025;75(1):10–45. doi:10.3322/caac.21871
3. Lam AK. Papillary Thyroid Carcinoma: current Position in Epidemiology, Genomics, and Classification. *Methods Mol Biol*. 2022;2534:1–15. doi:10.1007/978-1-0716-2505-7_1
4. Haugen BR, Alexander EK, Bible KC, et al. 2015 American Thyroid Association Management Guidelines for Adult Patients with Thyroid Nodules and Differentiated Thyroid Cancer: the American Thyroid Association Guidelines Task Force on Thyroid Nodules and Differentiated Thyroid Cancer. *Thyroid*. 2016;26(1):1–133. doi:10.1089/thy.2015.0020
5. Yang Y, Li S, Kkw T, Zhu S, Wang F, Fu L. Tumor-associated macrophages remodel the suppressive tumor immune microenvironment and targeted therapy for immunotherapy. *J Exp Clin Cancer Res*. 2025;44(1):145. doi:10.1186/s13046-025-03377-9
6. Vitale I, Shema E, Loi S, Galluzzi L. Intratumoral heterogeneity in cancer progression and response to immunotherapy. *Nat Med*. 2021;27(2):212–224. doi:10.1038/s41591-021-01233-9
7. Chmielik E, Rusinek D, Oczko-Wojciechowska M, et al. Heterogeneity of Thyroid Cancer. *Pathobiology*. 2018;85(1–2):117–129. doi:10.1159/000486422
8. Jia Q, Chu H, Jin Z, Long H, Zhu B. High-throughput single-cell sequencing in cancer research. *Signal Transduct Target Ther*. 2022;7(1):145. doi:10.1038/s41392-022-00990-4
9. Yan T, Qiu W, Weng H, Fan Y, Zhou G, Yang Z. Single-Cell Transcriptomic Analysis of Ecosystems in Papillary Thyroid Carcinoma Progression. *Front Endocrinol*. 2021;12:729565. doi:10.3389/fendo.2021.729565
10. Pu W, Shi X, Yu P, et al. Single-cell transcriptomic analysis of the tumor ecosystems underlying initiation and progression of papillary thyroid carcinoma. *Nat Commun*. 2021;12(1):6058. doi:10.1038/s41467-021-26343-3
11. Peng M, Wei G, Zhang Y, et al. Single-cell transcriptomic landscape reveals the differences in cell differentiation and immune microenvironment of papillary thyroid carcinoma between genders. *Cell Biosci*. 2021;11(1):39. doi:10.1186/s13578-021-00549-w
12. Wang T, Shi J, Li L, et al. Single-Cell Transcriptome Analysis Reveals Inter-Tumor Heterogeneity in Bilateral Papillary Thyroid Carcinoma. *Front Immunol*. 2022;13:840811. doi:10.3389/fimmu.2022.840811
13. Zheng G, Chen S, Ma W, et al. Spatial and Single-Cell Transcriptomics Unraveled Spatial Evolution of Papillary Thyroid Cancer. *Adv Sci*. 2025;12(2):e2404491. doi:10.1002/advs.202404491
14. Colombo M, Raposo G, Théry C. Biogenesis, secretion, and intercellular interactions of exosomes and other extracellular vesicles. *Annu Rev Cell Dev Biol*. 2014;30:255–289. doi:10.1146/annurev-cellbio-101512-122326
15. Kalluri R, LeBleu VS. The biology, function, and biomedical applications of exosomes. *Science*. 2020;367(6478):6977. doi:10.1126/science.aau6977
16. Pagni F, L'Imperio V, Bono F, et al. Proteome analysis in thyroid pathology. *Expert Rev Proteomics*. 2015;12(4):375–390. doi:10.1586/14789450.2015.1062369
17. Lin JD, Fu SS, Chen JY, et al. Clinical Manifestations and Gene Expression in Patients with Conventional Papillary Thyroid Carcinoma Carrying the BRAF(V600E) Mutation and BRAF Pseudogene. *Thyroid*. 2016;26(5):691–704. doi:10.1089/thy.2015.0044
18. Luo D, Zhan S, Xia W, Huang L, Ge W, Wang T. Proteomics study of serum exosomes from papillary thyroid cancer patients. *Endocr Relat Cancer*. 2018;25(10):879–891. doi:10.1530/erc-17-0547
19. Huang TY, Wang CY, Chen KY, Huang LT. Urinary Exosomal Thyroglobulin in Thyroid Cancer Patients With Post-ablative Therapy: a New Biomarker in Thyroid Cancer. *Front Endocrinol*. 2020;11:382. doi:10.3389/fendo.2020.00382
20. Zhou JK, Fan X, Cheng J, Liu W, Peng Y. PDLIM1: structure, function and implication in cancer. *Cell Stress*. 2021;5(8):119–127. doi:10.15698/cst2021.08.254
21. Chen HN, Yuan K, Xie N, et al. PDLIM1 Stabilizes the E-Cadherin/β-Catenin Complex to Prevent Epithelial-Mesenchymal Transition and Metastatic Potential of Colorectal Cancer Cells. *Cancer Res*. 2016;76(5):1122–1134. doi:10.1158/0008-5472.Can-15-1962
22. Huang Z, Zhou JK, Wang K, et al. PDLIM1 Inhibits Tumor Metastasis Through Activating Hippo Signaling in Hepatocellular Carcinoma. *Hepatology*. 2020;71(5):1643–1659. doi:10.1002/hep.30930
23. Liu Z, Zhan Y, Tu Y, Chen K, Liu Z, Wu C. PDZ and LIM domain protein 1(PDLIM1)/CLP36 promotes breast cancer cell migration, invasion and metastasis through interaction with α-actinin. *Oncogene*. 2015;34(10):1300–1311. doi:10.1038/onc.2014.64
24. Hong SH. Identification of CLP36 as a tumor antigen that induces an antibody response in pancreatic cancer. *Cancer Res Treat*. 2005;37(1):71–77. doi:10.4143/crt.2005.37.1.71
25. Ahn BY, Saldanha-Gama RF, Rahn JJ, et al. Glioma invasion mediated by the p75 neurotrophin receptor (p75(NTR)/CD271) requires regulated interaction with PDLIM1. *Oncogene*. 2016;35(11):1411–1422. doi:10.1038/onc.2015.199
26. Li LM, Luo FJ, Song X. MicroRNA-370-3p inhibits cell proliferation and induces chronic myelogenous leukaemia cell apoptosis by suppressing PDLIM1/Wnt/β-catenin signaling. *Neoplasma*. 2020;67(3):509–518. doi:10.4149/neo_2020_190612N506
27. Ye B, Yu M, Yue M, et al. Role of PDLIM1 in hepatic stellate cell activation and liver fibrosis progression. *Sci Rep*. 2023;13(1):10946. doi:10.1038/s41598-023-38144-3

28. Wei X, Zhang Y, Yu S, et al. PDLIM5 identified by label-free quantitative proteomics as a potential novel biomarker of papillary thyroid carcinoma. *Biochem Biophys Res Commun*. 2018;499(2):338–344. doi:10.1016/j.bbrc.2018.03.159
29. Sun D, Guan X, Moran AE, et al. Identifying phenotype-associated subpopulations by integrating bulk and single-cell sequencing data. *Nat Biotechnol*. 2022;40(4):527–538. doi:10.1038/s41587-021-01091-3
30. Gerstberger S, Jiang Q, Ganesh K. Metastasis. *Cell*. 2023;186(8):1564–1579. doi:10.1016/j.cell.2023.03.003
31. Massagué J, Ganesh K. Metastasis-Initiating Cells and Ecosystems. *Cancer Discov*. 2021;11(4):971–994. doi:10.1158/2159-8290.Cd-21-0010
32. Li C, Hou X, Zhang P, et al. Exosome-based Tumor Therapy: opportunities and Challenges. *Curr Drug Metab*. 2020;21(5):339–351. doi:10.2174/1389200221666200515103354
33. Sharma A, Johnson A. Exosome DNA: critical regulator of tumor immunity and a diagnostic biomarker. *J Cell Physiol*. 2020;235(3):1921–1932. doi:10.1002/jcp.29153
34. Li C, Zhou T, Chen J, et al. The role of Exosomal miRNAs in cancer. *J Transl Med*. 2022;20(1):6. doi:10.1186/s12967-021-03215-4
35. Hoshino A, Costa-Silva B, Shen TL, et al. Tumour exosome integrins determine organotropic metastasis. *Nature*. 2015;527(7578):329–335. doi:10.1038/nature15756
36. Alnaqbi H, Becker LM, Mousa M, et al. Immunomodulation by endothelial cells: prospects for cancer therapy. *Trends Cancer*. 2024;10(11):1072–1091. doi:10.1016/j.trecan.2024.08.002
37. Aydoğdu YF, Gülçek E, Büyükkasap Ç, Bostancı H. Outcomes of thyroidectomy for secondary thyroid malignancies, a single center experience. *Discov Oncol*. 2024;15(1):104. doi:10.1007/s12672-024-00967-5
38. Ono R, Kaisho T, Tanaka T. PDLIM1 inhibits NF-κB-mediated inflammatory signaling by sequestering the p65 subunit of NF-κB in the cytoplasm. *Sci Rep*. 2015;5:18327. doi:10.1038/srep18327
39. Wang H, Shi J, Luo Y, et al. LIM and SH3 protein 1 induces TGFβ-mediated epithelial-mesenchymal transition in human colorectal cancer by regulating S100A4 expression. *Clin Cancer Res*. 2014;20(22):5835–5847. doi:10.1158/1078-0432.Ccr-14-0485
40. Kim W, Khan SK, Gvozdenovic-Jeremic J, et al. Hippo signaling interactions with Wnt/β-catenin and Notch signaling repress liver tumorigenesis. *J Clin Invest*. 2017;127(1):137–152. doi:10.1172/jci88486
41. Zhang M, Wang W. Organization of signaling complexes by PDZ-domain scaffold proteins. *Acc Chem Res*. 2003;36(7):530–538. doi:10.1021/ar020210b
42. Zhao R, Bei X, Yang B, et al. Endothelial cells promote metastasis of prostate cancer by enhancing autophagy. *J Exp Clin Cancer Res*. 2018;37(1):221. doi:10.1186/s13046-018-0884-2
43. Kim N, Kim HK, Lee K, et al. Single-cell RNA sequencing demonstrates the molecular and cellular reprogramming of metastatic lung adenocarcinoma. *Nat Commun*. 2020;11(1):2285. doi:10.1038/s41467-020-16164-1
44. Broggi MAS, Maillat L, Clement CC, et al. Tumor-associated factors are enriched in lymphatic exudate compared to plasma in metastatic melanoma patients. *J Exp Med*. 2019;216(5):1091–1107. doi:10.1084/jem.20181618
45. García-Silva S, Benito-Martín A, Sánchez-Redondo S, et al. Use of extracellular vesicles from lymphatic drainage as surrogate markers of melanoma progression and BRAF (V600E) mutation. *J Exp Med*. 2019;216(5):1061–1070. doi:10.1084/jem.20181522